Tropical Atlantic salinity variability: New insights from SMOS

E. Tzortzi,[1,2] S. A. Josey,[1] M. Srokosz,[1] and C. Gommenginger[1]

[1] Observations from the SMOS satellite are used to reveal new aspects of Tropical Atlantic sea surface salinity (SSS) variability. Over an annual cycle, the variability is dominated by eastern and western basin SSS "poles," with seasonal ranges up to 6.5 pss (practical salinity scale), that vary out of phase by 6 months and largely compensate each other. A much smaller SSS range (0.08 pss) is observed for the region as a whole. The dominant processes controlling SSS variability are investigated using GPCPv2.2 precipitation (P), OAFlux evaporation (E), and Dai and Trenberth river flow (R) data sets. For the western pole, SSS varies in phase with P and lags R by 1–2 months; a more complex relationship holds for the eastern pole. The synthesis of novel satellite SSS data with E, P, and R enables a new approach to determining variability in Tropical freshwater fluxes and its potential impacts on the Atlantic ocean circulation. **Citation:** Tzortzi, E., S. A. Josey, M. Srokosz, and C. Gommenginger (2013), Tropical Atlantic salinity variability: New insights from SMOS, *Geophys. Res. Lett., 40,* 2143–2147, doi:10.1002/grl.50225.

1. Introduction

[2] Sea surface salinity (SSS) is a natural indicator of changes in the hydrological cycle [*IPCC*, 2007; *Bindoff et al.*, 2007; *Yu*, 2011]. Salinity variations in recent decades [*Curry et al.*, 2003; *Terray et al.*, 2012; *Durack et al.*, 2012] have been linked to the Atlantic meridional overturning circulation (MOC) strength and variability [*Thorpe et al.*, 2001; *Häkkinen*, 2002; *Vellinga and Wu*, 2004; *Wang et al.*, 2010]. The Tropical Atlantic is potentially important for the strength of the MOC via its influence on the salinity of waters advected to dense water formation regions [*Vellinga et al.*, 2002; *Pardaens et al.*, 2008]. However, a historical lack of in situ observations has prevented a reliable depiction of SSS variability in this region [*Delcroix et al.*, 2005; *Reverdin et al.*, 2007; *Gordon and Giulivi*, 2008].

[3] The recent advent of L-band satellite SSS measurements from the European Space Agency Soil Moisture and Ocean Salinity (SMOS) mission, launched in November 2009, provides a new opportunity to determine Tropical Atlantic SSS variability. The SMOS and more recent Aquarius/SACD salinity missions have started to provide new insights into SSS-related processes, for example, the eastern Pacific fresh pool [*Alory et al.*, 2012], hurricanes [*Reul et al.*, 2012a; *Grodsky et al.*, 2012], and Tropical Instability Waves [*Lee et al.*, 2012; *Lagerloef et al.*, 2012].

[4] We present here the first analysis of SSS variability at seasonal time scales in the Tropical Atlantic using data from SMOS. The salinity balance in this region is expected to be influenced by variations in precipitation and evaporation associated with the north-south movement of the Inter-Tropical Convergence Zone (ITCZ) and outflow from two of the largest global river systems: the Amazon/Orinoco and Niger/Congo. We use SMOS SSS observations in combination with the latest version of the GPCP precipitation (P), the OAFlux evaporation (E), and the Dai and Trenberth river flow (R) data sets to determine SSS changes throughout the annual cycle and investigate the key processes that control this variability.

[5] Previous analyses based on ship data are heavily limited by the concentration of data along a few narrow shipping routes and near-complete lack of information in between (see, e.g., Figure 1 of *Dessier and Donguy*, [1994]). Such analyses provide some indication of the influence of river outflow on salinity but are necessarily climatological in nature and only provide a "very crude picture of the SSS field" [*Dessier and Donguy*, 1994]. SMOS offers a major step forward as, for the first time, it is possible to quantify salinity variability using spatially complete fields for individual years rather than relying on heavily interpolated climatological data sets with significant sampling issues. The data sets that we employ are described in section 2, and our novel results are presented in section 3. This is followed by a discussion of their significance and conclusions in section 4.

2. Data Sets

[6] For this study, we use research SMOS SSS level 3 monthly mean products (V01) for the first complete year (2010) at $1.0° \times 1.0°$ spatial resolution from the French Centre Aval de Traitement des Donnees SMOS (CATDS) [*Reul et al.*, 2011]. The uncertainty of SMOS SSS in individual $1.0°$ grid cells in the Tropics has been estimated to be around 0.3 pss (practical salinity scale) [*Reul et al.*, 2012b]. Monthly P fields for the same period have been taken from the latest satellite-gauge product of the Global Precipitation Climatology Project (GPCP), version 2.2 [*Huffman and Bolvin*, 2012] released in August 2012, at $2.5° \times 2.5°$ resolution. Monthly E fields are acquired from the Objectively Analyzed air-sea Fluxes (OAFlux) hybrid data set [*Yu and Weller*, 2007; *Yu et al.*, 2008], which has a $1.0° \times 1.0°$ spatial resolution and is a combination of satellite and reanalysis data. Finally, time series of monthly river flow rates at the farthest downstream station for the Amazon, Orinoco, Congo, and Niger rivers are obtained from the Dai and Trenberth Global River Flow Dataset [*Dai and Trenberth*, 2002; *Dai et al.*, 2009]. These are used to form climatological means for the common period of January 1941 to December 1992 when data are available for all four rivers. In addition, we have used data for 2010 from

[1]National Oceanography Centre Southampton, Southampton, UK.
[2]School of Ocean and Earth Science, University of Southampton, Southampton, UK.

Corresponding author: E. Tzortzi, Room 164/25, National Oceanography Centre, European Way, Southampton SO14 3ZH, UK. (E.Tzortzi@noc.soton.ac.uk)

the ORE-HYBAM network stations (www.ore-hybam.org) for the Amazon and Orinoco rivers. Note that data from this source are not available for the Niger so we are not able to include them in our eastern subregion analysis.
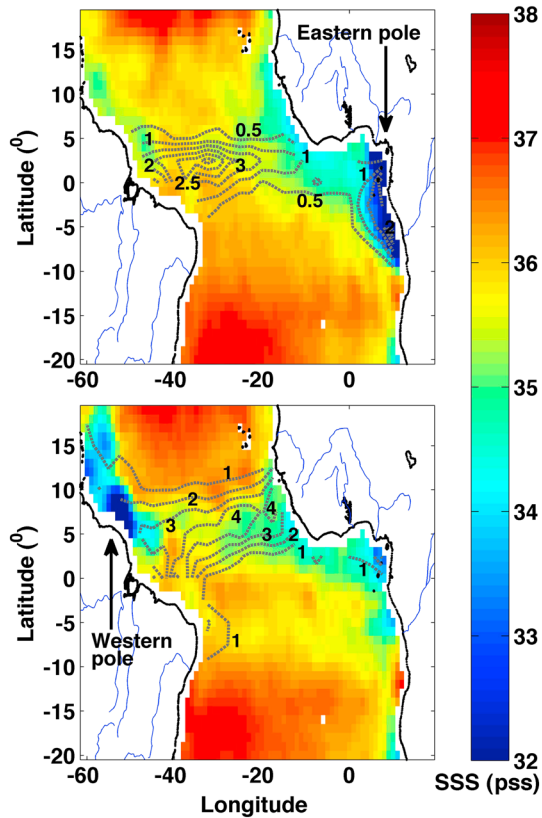
3. Results

3.1. SSS Variability in the Tropical Atlantic from SMOS

[7] Monthly mean fields of SSS from SMOS in the Tropical Atlantic are shown in Figure 1 for January and July 2010. SSS displays its highest values at the northern and southern extremes of this region throughout the year, reaching up to ~37.4 pss. In contrast, in the equatorial band, SSS is reduced, varying around 34.5–35.0 pss, and the location of this band is displaced northward in July relative to January. This is consistent with the northward displacement of the ITCZ and hence the zone of maximum P in boreal summer, as shown by the contours in Figure 1.

[8] By combining SMOS data with the latest version of the GPCP satellite precipitation data set and evaporation from OAFlux, we are able to carry out an observation-based comparison of these terms for individual months in 2010 (zonal means for January and July are shown in Figure 2, where the average at a given latitude is taken across the width of the basin). There is a clear alignment between the SSS minimum and the maximum (minimum) in P (E-P), indicating that at basin wide scales the position of the salinity minimum is tied to the precipitation maximum (the variation in E is relatively small across the Tropics). This is the first time that such an analysis has been possible using satellite data alone for the two principal fields (SSS and P) and demonstrates the ability of remote sensing for tracking variability in these key components of the Tropical freshwater budget.

[9] In addition, the SMOS data reveal the presence of seasonally dependent SSS minima (referred to hereafter as "poles") on opposite sides of the basin located north/south of the equator in the western/eastern basin (see Figure 1). These poles are close to the outflows of the major river systems, and previous analyses of climatological ship observation-based data sets suggest that outflow plays a significant role in their generation [*Dessier and Donguy*, 1994]. In the western Tropical Atlantic pole, the fresh signal is stronger in July (SSS as low as 29.7 pss) than January (SSS minimum ~35.0 pss). In contrast, the eastern Tropical Atlantic pole in the Gulf of Guinea has its lowest salinity in January (SSS ~28.8 pss) and is more saline in July (minimum 33.5 pss).

Figure 1. SMOS SSS mean (pss) in the Tropical Atlantic for (top) January and (bottom) July 2010, with GPCP P mean contours (m/year) overlaid. Note that P contours for January are shown every 0.5 m/year, while those for July are every 1 m/year (to avoid overcrowding of contour lines).
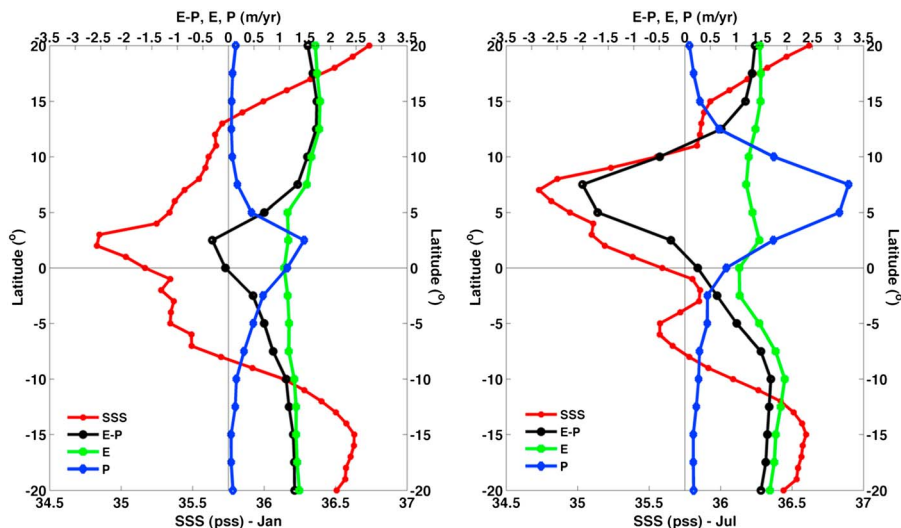

Figure 2. Tropical Atlantic zonal mean values for (red) SSS, (green) E, (blue) P, and (black) E-P for (left panel) January 2010 and (right panel) July 2010. The zonal mean at a given latitude is taken across the width of the basin.

[10] The two salinity poles are clearly evident in Figure 3, which shows the seasonal range of SSS in 2010 (i.e., the difference between the maximum and minimum monthly mean values in each grid cell). The magnitude of the range in each pole is similar, up to 6.5 (6) pss in the eastern (western) Tropical Atlantic. In contrast, the SSS seasonal range typically lies between 0.1 and 1.5 pss for the rest of the region.

[11] We have quantified the area-weighted mean SSS for subregions that encompass the two poles defined according to the criterion that the seasonal range in SSS exceeds 1.5 pss (different choices for this threshold have been considered and do not significantly modify our conclusions). These subregions are indicated by the areas outlined in black in Figure 3. The seasonal cycle of SSS for these two subregions, and the region from 20°N–20°S as a whole, is shown in Figure 4. SSS is typically fresher in the eastern subregion and has a slightly
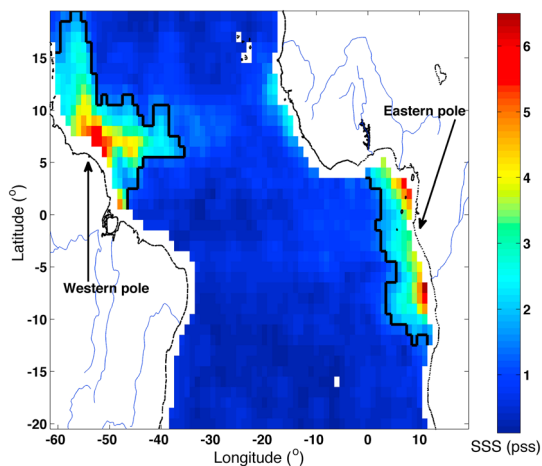

Figure 3. SMOS SSS range (maximum minus minimum during the year) in the Tropical Atlantic 20°N–20°S for 2010. The solid black lines indicate the boundaries of the western and eastern subregions defined according to the condition that the seasonal range in SSS is greater than 1.5 pss.
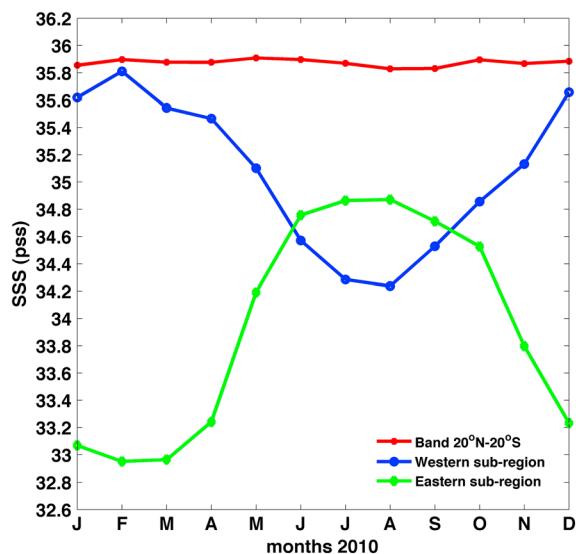

Figure 4. Area-weighted mean of SMOS SSS (pss) over (red) the whole region 20°N–20°S, (blue) the western subregion, and (green) the eastern subregion in 2010.

larger seasonal variability (here by ~0.35 pss) compared to the western subregion. The subregions are characterized by out-of-phase seasonal cycles and tend to compensate as the mean SSS for the whole region shows little seasonal variation. The seasonal range for the eastern subregion is 1.92 pss, for the western subregion is 1.57 pss, and for the region as a whole is 0.08 pss.

3.2. Relationship of SSS Variability to E, P, and R

[12] We now examine the extent to which the strong seasonal variability in SSS revealed by SMOS in the eastern and western subregions may be linked to variations in surface freshwater forcing due to evaporation, precipitation, and runoff. For this analysis, we focus on the phase relationships between the seasonal cycles of the different terms. This is supported by estimates of the relative magnitudes of the E, P, and R seasonal ranges (obtained by integrating over the relevant subregions in the case of E and P). The seasonal cycles of SSS, E-P, E, P, and R in each subregion are shown in Figure 5. In addition to climatological R, Figure 5 includes river discharge for 2010 obtained from the ORE-HYBAM network stations for the Amazon and Orinoco rivers in the western subregion.

[13] In the western subregion, strong seasonal cycles are evident in SSS, P, E-P, and R. SSS varies in phase with P, and lags R by about 1 month. To show the phase relationships more clearly, vertical lines on the figure indicate the months of maximum (February) and minimum (August) SSS. These coincide with the minimum and maximum months of the P cycle and lag the minimum (maximum) in R by 2 (1) months. In contrast to the other terms, E is relatively constant throughout the year and is thus unlikely to play a significant role in the strong SSS variability observed by SMOS. Consequently, the E-P seasonal cycle closely follows the variation found for P alone. The amplitudes of the E-P and R seasonal cycles are similar in magnitude implying a roughly equal contribution of variability in the air-sea freshwater flux (dominated by P) and the river outflow, R, to the seasonal variability in SSS. Caveats that need to be borne in mind here are that the R data are climatological in nature and that mixing and advective processes have been ignored. Note that the ORE-HYBAM data for R in 2010 show the same maximum and minimum months as the climatological data, indicating that our phase relationship conclusions drawn above are not affected by the use of climatological data for R. The amplitude of the cycle is larger than the climatological range, indicating a potentially more significant role for R in this particular year relative to the long-term mean.

[14] Seasonal cycles in all terms are observed in the eastern subregion as E now has a clearer seasonal variation than in the western subregion, although its amplitude remains smaller than P. The clear in-phase relationship between SSS and P observed in the western subregion is no longer evident. The maximum in SSS falls within a prolonged 4 month period, July–September, in which P is at a minimum. However, the SSS minimum in February occurs at a time when P is close to the average for the year as a whole, and at this time, P exhibits strong intermonth variability. The intermonth variability may reflect limitations with the satellite data set as the eastern subregion is more coastally confined than the western subregion and the accuracy of the GPCPv2.2 precipitation retrievals are potentially influenced by the proximity of land.
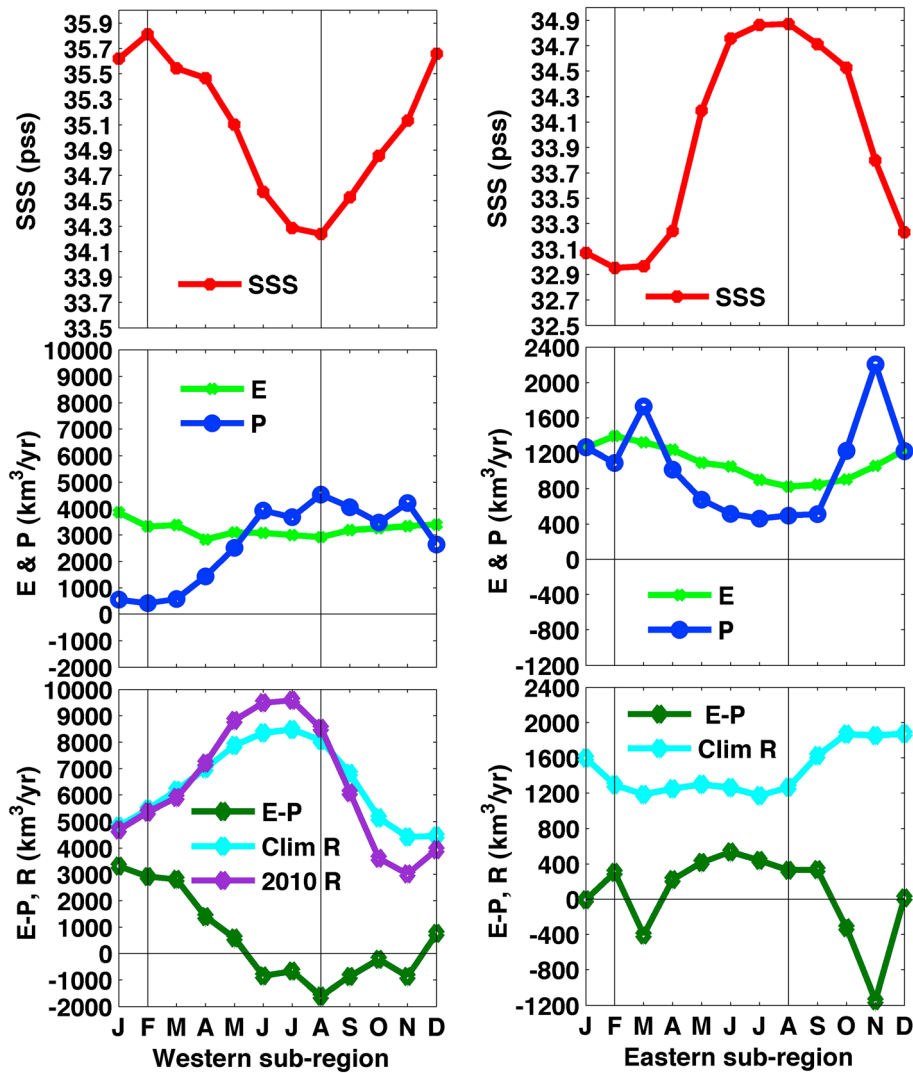
Figure 5. Seasonal cycles for 2010 of (red) area-weighted mean SMOS SSS and (light green) integrated OAFlux E, (blue) GPCP P, and (dark green) OAFLUX-GPCP E-P for the western subregion (left panel) and the eastern subregion (right panel). Also shown are the sum of the long-term climatological means of riverine flow rates (R, cyan lines) for the period 1941–1992 for the (bottom left panel) Amazon and Orinoco in the western subregion and (bottom right panel) Congo and Niger in the eastern subregion. Finally, ORE-HYBAM monthly river dicharge data for 2010 for the Amazon and Orinoco in the western subregion are shown in purple.

The relationship between SSS and R in the eastern subregion is also unclear as both the SSS maximum and minimum months have similar values for R (although there is some consistency as the SSS maximum falls at the end of a prolonged period, March–July, of low river outflow). The difference in strength of the SSS-R phase relationship between the two subregions may arise from the considerably lower outflow rates in the Congo/Niger river system (about 1500 km^3 year^{-1}) compared to the Amazon/Orinoco (about 7000 km^3 year^{-1}) that are likely to result in a weaker impact on SSS.

[15] In summary, the western subregion shows a clear relationship between SSS, P, and R with in-phase agreement between SSS and P and a 1–2 month lag of SSS with respect to R. The relationships in the eastern subregion are not well defined, and this may reflect a weaker R signal. In both cases, a more detailed treatment of the budgets, which takes into account advection and mixing, is required to make further progress.

4. Summary and Conclusions

[16] Analyses of ocean surface salinity variability to date have been severely limited by the lack of data as they have relied primarily on irregular, spatially inhomogeneous measurements from ships [e.g., *Dessier and Donguy*, 1994]. With the advent of spatially dense salinity measurements from space through the SMOS and Aquarius/SACD satellites, it is now possible to characterize sea surface salinity (SSS) variability in more detail to investigate the processes that drive it. We presented here the first satellite-based analysis of SSS variability at seasonal time scales in the Tropical Atlantic using the first full year, 2010, of SMOS measurements. Our results show that, in the Tropical Atlantic at least, the SMOS SSS data from CATDS are of sufficient quality to provide valuable scientific insight into processes governing SSS variability.

[17] The Tropical Atlantic has a relatively constant salinity throughout the year during 2010 varying by just 0.08 pss when averaged over the region as a whole. However, strong local variations are evident at two poles on opposite sides of the basin that are close to the outflows from the Amazon/ Orinoco and Congo/Niger river systems. The SMOS measurements reveal large amplitude seasonal cycles up to 6.5 pss at these two sites that are out of phase by 6 months and compensate each other in their influence on the whole region's mean salinity. The relationships between these seasonal cycles and the surface forcing terms—E, P, and R—were investigated. For the western pole, SSS varies in phase with P, while it lags R by 1–2 months (E has little seasonal variability). In contrast, it is difficult to establish a clear relationship between SSS and the surface forcing terms for the eastern pole, and this may indicate a significant role for advection and mixing [*Yu*, 2011]. We plan to undertake a more detailed treatment of the budgets that takes into account advection and mixing in future research.

[18] Further analysis of the developing data record from SMOS, supplemented by Aquarius/SACD and Argo float data (which provide useful complementary information on surface salinity but do not achieve the spatial and temporal sampling possible using satellites), will reveal whether the seasonal compensation between the two poles continues to hold at multiannual time scales. The amplitude of the seasonal cycle in SSS for the full region doubles to about 0.16 pss if either pole is excluded from the full regional mean, indicating the sensitivity of the Tropical Atlantic salinity budget to their influence. Variations in the amplitude or phasing of the salinity variability in either pole thus have the potential to significantly modify Tropical Atlantic SSS with consequences for higher-latitude Atlantic circulation through modified surface layer density [*Vellinga and Wu*, 2004]. Such variations may be expected as result of natural variability (e.g., through the influence of El Niño) and anthropogenic climate change. To conclude, the novel results presented here clearly demonstrate (1) the potential of harnessing satellite-based SSS and P observations to develop our understanding of controls on ocean surface salinity and (2) their value in monitoring salinity variability over Tropical regions that have the potential to influence the larger-scale ocean circulation.

References

Alory, G., C. Maes, T. Delcroix, N. Reul, and S. Illig (2012), Seasonal dynamics of sea surface salinity off Panama: The far eastern Pacific fresh pool, *J. Geophys. Res.*, *117*, C04028, doi:10.1029/2011JC007802.

Bindoff, N. L., et al. (2007), Observations: Oceanic climate change and sea level, in *Climate Change 2007: The Physical Science Basis: Contribution of Working Group I to the Fourth Assessment Report of the Intergovernmental Panel on Climate Change*, edited by S. Solomon et al., pp. 385–432, Cambridge University Press, New York.

Curry, R., R. R. Dickson, and I. Yashayaev (2003), A change in the fresh water balance of the Atlantic over the past four decades, *Nature*, *426* (6968), 826–829.

Dai, A., and K. E. Trenberth (2002), Estimates of freshwater discharge from continents: Latitudinal and seasonal variations, *J. Hydrometeorol.*, *3*, 660–687.

Dai, A., T. Qian, K. E. Trenberth, and J. D. Milliman (2009), Changes in continental freshwater discharge from 1948 to 2004, *J. Climate*, *22*, 2773–2792.

Delcroix, T., M. McPhaden, A. Dessier, and Y. Gouriou (2005), Time and space scales for sea surface salinity in the Tropical oceans, *Deep Sea Res., Part I*, *52*, 787–813.

Dessier, A., and J. R. Donguy (1994), The sea surface salinity in the tropical Atlantic between 10° S and 30° N - Seasonal and interannual variations (1977–1989), *Deep Sea Res., Part I*, *41*, 81–100, doi:10.1016/0967-0637 (94)90027-2.

Durack, P. J., S. E. Wijffels, and R. J. Matear (2012), Ocean salinities reveal strong global water cycle intensification during 1950 to 2000, *Science*, *336*, 455–458, doi:10.1126/science.1212222.

Gordon, A. L., and C. F. Giulivi (2008), Sea surface salinity trends over fifty years within the subtropical North Atlantic, *Oceanography*, *21*(1a), 20–29.

Grodsky, S. A., N. Reul, G. Lagerloef, G. Reverdin, J. A. Carton, B. Chapron, Y. Quilfen, V. A. Kudryavtsev, and H.-Y. Kao (2012), Haline hurricane wake in the Amazon/Orinoco plume: AQUARIUS/SACD and SMOS observations, *Geophys. Res. Lett.*, *39*, doi:10.1029/2012GL053335.

Häkkinen, S. (2002), Surface salinity in the northern North Atlantic, *J. Geophys. Res.*, *107* (C12), 8003, doi:10.1029/2001JC00081.

Huffman, G. J., and D. T. Bolvin (2012), GPCP Version 2.2 Combined Precipitation Data Set Documentation, Laboratory for Atmospheres, NASA, 27 August 2012, ftp://precip.gsfc.nasa.gov/pub/gpcp-v2.2/doc/V2.2_doc.pdf.

Intergovernmental Panel on Climate Change (IPCC) (2007), *Climate Change: The Physical Science Basis*, edited by S. Solomon, D. Qin, M. Manning, Z. Chen, M. Marquis, K. B. Avery, M. Tignor, and H. L. Miller, Cambridge University Press, Cambridge, UK.

Lagerloef, G., F. Wentz, S. Yueh, H-Y. Kao, G. C. Johnson, and J. M. Lyman (2012), Aquarius satellite mission provides new, detailed view of sea surface salinity, *Bull. Am. Meteorol. Soc.*, *93* (7), S70–S71, doi:10.1175/ 2012BAMSStateoftheClimate.1.

Lee, T., G. Lagerloef, M. M. Gierach, H.-Y. Kao, S. Yueh, and K. Dohan (2012), Aquarius reveals salinity structure of Tropical instability waves, *Geophys. Res. Lett.*, *39*, L12610, doi:10.1029/2012GL052232.

Pardaens, A., M. Vellinga, P. Wu, and B. Ingleby (2008), Large-scale Atlantic salinity changes over the last half-century: A model–observation comparison, *J. Climate*, *21*, 1698–1720.

Reul, N., and Ifremer CATDS-CECOS Team (2011), SMOS L3 SSS Research Products: Product User Manual Reprocessed Year 2010, IFREMER, Plouzané, France.

Reul, N., J. Tenerelli, B. Chapron, D. Vandemark, Y. Quilfen, and Y. Kerr (2012a), SMOS satellite L-band radiometer. A new capability for ocean surface remote sensing in hurricanes, *J. Geophys. Res. Oceans*, *117*, C02006, doi:10.1029/2011JC007474.

Reul, N., J. Tenerelli, J. Boutin, B. Chapron, F. Paul, E. Brion, F. Gaillard, and O. Archer (2012b), Overview of the first SMOS sea surface salinity products. Part I: Quality assessment for the second half of 2010, *IEEE Trans. Geosci. Remote Sens.*, *50*, 1636–1647, doi:10.1109/ TGRS.2012.2188408.

Reverdin, G., E. Kesterane, C. Frankignoul, and T. Delcroix (2007), Sea surface salinity in the Atlantic Ocean (30°S-50°N), *Prog. Oceanogr.*, *73*, 311–340, doi:10.1026/j.pocean.2006.11.004.

Terray, L., L. Corre, S. Cravatte, T. Delcroix, G. Reverdin, and A. Ribes (2012), Near-surface salinity as nature's rain gauge to detect human influence on the Tropical water cycle, *J. Climate*, *25*, 958–977.

Thorpe, R. B., J. M. Gregory, T. C. Johns, R. A. Wood, and J. F. B. Mitchell (2001), Mechanisms determining the Atlantic thermohaline circulation response to greenhouse gas forcing in a non-flux-adjusted coupled climate model, *J. Climate*, *14*, 3102–3116.

Vellinga, M., R. A. Wood, and J. M. Gregory (2002), Processes governing the recovery of a perturbed thermohaline circulation HadCM3, *J. Climate*, *15*, 764–780.

Vellinga, M., and P. Wu (2004), Low-latitude fresh water influence on centennial variability of the thermohaline circulation, *J. Climate*, *17*, 4498–4511.

Wang, C., S. Dong, and E. Munoz (2010), Seawater density variations in the North Atlantic and the Atlantic meridional overturning circulation, *Clim. Dyn.*, *34*, 953–968.

Yu, L., and R. Weller (2007), Objectively analyzed air–sea heat fluxes for the global ice-free oceans (1981–2005), *Bull. Am. Meteorol. Soc.*, *88*, 527–539.

Yu, L., X. Jin, and R. A. Weller (2008), Multidecade Global Flux Datasets from the Objectively Analyzed Air-sea Fluxes (OAFlux) Project: Latent and Sensible Heat Fluxes, Ocean Evaporation, and Related Surface Meteorological Variables, Technical Report OAFlux Project Technical Report (OA2008-01), Woods Hole Oceanographic Institution, http:// oaflux.whoi.edu/publications.html.

Yu, L. (2011), A global relationship between the ocean water cycle and near-surface salinity, *J. Geophys. Res.*, *116*, C10025, doi:10.1029/ 2010JC006937.